Cryst. Res. Technol.	34	1999	5–6	719–728

S.M. KACZMAREK, R. JABLONSKI*, Z. MOROZ**, I. PRACKA*,
T. LUKASIEWICZ*

Military University of Technology
*Institute of Electronic Materials Technology
**Soltan Institute of Nuclear Studies, Poland

Radiation Defects in Oxide Compounds

Yttrium-aluminum garnets, strontium and barium lanthanum gallates, lithium niobate and tantalate as-grown crystals and doped by diffusion with rare-earth (Nd, Dy, Er, Tm, Ho, Pr, Ce) and metal transition elements (Mn, Cr) were investigated optically and using Electron Spin Resonance method before and after gamma, electron and proton irradiation.

Keywords: gamma; proton and electron irradiations; additional absorption; electron spin resonance; radiation defects; oxide compounds

1. Introduction

Among many defects arising during the crystal growth of oxide compounds, a variety of defects are observed: facets, growth striations, dislocations, low angle boundaries, twins, color centers , dislocations with strain field, vacancies, cellular structure, inclusions and cracks (PAJACZKOWSKA 1995). Among these defects, point defects in a given crystal can be sources of new, radiation defects during its application in devices working in external radiation fields. Output characteristics of these devices changes (e.g. lasers) in an obvious manner. However, positive effect of radiation defects on output characteristics of some materials is also known (BEDILOV et al. 1994, KACZMAREK et al. 1995).

It is difficult to define the nature of color centers. Sometimes these defects are related to impurities although their level may be lower than 10^{-6} weight % while sometimes they are due to oxygen nonstoichiometry or change in cation balance.

The main purpose of the present work was to determine the radiation induced defects in $Y_3Al_5O_{12}$ (YAG), $SrLaAlO_4$ (SLAO), $SrLaGaO_4$ (SLGO4), $CaNdAlO_4$ (CNAO), $SrLaGa_3O_7$ (SLGO), $BaLaGa_3O_7$ (BLGO), $LiTaO_3$ (LT) and $LiNbO_3$ (LN) single crystals doped with rare-earth and ions of the first transition series.

2. Experimental

The ESR spectra of the single crystals were recorded at 9.4 GHz in the temperature range from 4 K to 300 K using a BRUKER ESP -300 X-band spectrometer. The absorption spectra were taken at 300 K in the spectral range between 4500 and 500 cm^{-1} using a FTIR spectrometer (IFS 113V BRUKER) and in the range 190-1100 nm using a LAMBDA 2 spectrometer (Perkin-Elmer). ESR and optical measurements were made before and after the samples were exposed to ionizing radiation.

Three different sources of radiation were used: (1) γ-irradiation at 300 K and 77K, (2) electrons with fluencies 10^{14} - 5 x 10^{16} electrons/cm^2 at 77 K, and (3) protons with fluencies

10^{13} - 10^{16} protons/cm^2. The gamma ray irradiation of the samples was performed with a ^{60}Co source at a rate of 1.5 Gy/s up to an absorbed dose of 10^5 Gy. Electron irradiations at an energy of 1 MeV were performed using a Van de Graaf accelerator. Proton exposures were done with the use of a C30 cyclotron at an energy of 21 MeV. Values of $\Delta K(\lambda)$ factors which describe an additional absorption due to the irradiation were calculated according to the formula:

$$\Delta K(\lambda) = \frac{1}{d} \cdot \ln \frac{T_1}{T_2}, \tag{1}$$

where K is absorption, $\Delta K(\lambda)$ is the additional absorption, λ is the wavelength, d is the sample thickness, and T_1 and T_2 are the transmissions of the sample measured before and after irradiation, respectively.

3. Color centers in $ABCO_4$ crystals

Lanthanum gallate and lanthanum aluminate seem to be suitable substrates for thin film epitaxial growth of the high temperature superconductors $YBa_2Cu_3O_{7-d}$ and $La_{2-x}Sr_xCuO_4$ (PAJACZKOWSKA et al. 1995). The interest in these materials stems from their crystal structure, lattice constant and dielectric properties. Thus changes in their structure under influence of external field, e.g. thermal and radiation, are very important observations for a later application.

Both SLGO4 and SLAO crystallize in a tetragonal structure similar to that of K_2NiF_4. Crystal lattices contain linked oxygen octahedrally with Al or Ga ions in their center and with Sr and La ions located between them. Therefore, each Al or Ga ion has six oxygen ions in their first coordination zone and nine Sr or La ions in their second coordination zone. Additionally, it is usually assumed that Sr and La are random distributed between oxygen octahedra.

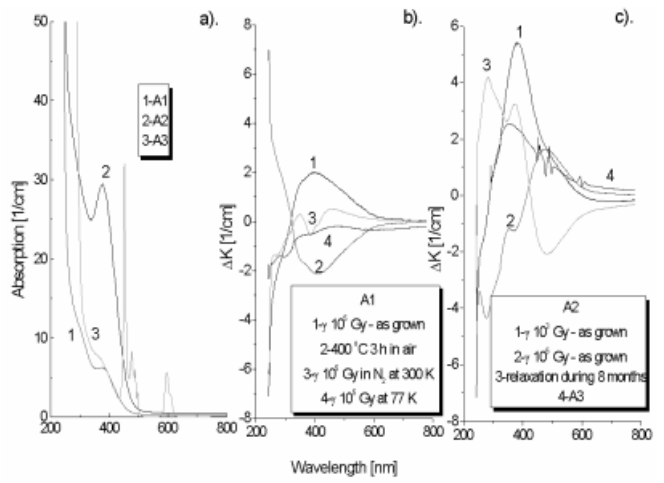

Fig. 1: (a) absorption and (b, c) additional absorption in pure (A1 and A2 samples) and Pr^{3+} (6 at.%) doped (A3 sample) $SrLaAlO_4$ single crystals after γ-irradiation with doses 10^3-10^5 Gy. Irradiation were performed on as grown crystals: in air at 300 K (curve 1, Fig. 1b and curves 1,2 and 4 in Fig. 1c), in N_2 gas at 300 K (curve 3, Fig. 1b) and in N_2 liquid at 77 K (curve 4, Fig. 1b)

Fig. 1 presents additional absorption bands in two undoped SLAO samples (A1 and A2 samples) coming from two different crystal growth runs and an SLAO sample doped with Pr^{3+} - 6 at.% - A3 sample. The γ-irradiation were performed on as grown crystals: in air at 300 K (curve 1, Fig. 1b and curves 1,2 and 4 in Fig. 1c), in N_2 gas at 300 K (curve 3, Fig.

1b) and in N_2 liquid at 77 K (curve 4, Fig. 1b). As seen from curves 1 and 2 in the Fig. 1a, undoped SLAO exhibit different value of absorption spectrum with maximum at 381 nm, equal to 5.5 and 30 cm^{-1} for samples 1 and 2, respectively, although additional absorption after γ-irradiation with a dose of 10^5 Gy is the same (2 cm^{-1}) - see curve 1 in Fig. 1b and curve 2 in Fig. 1c. Moreover, the shape of the additional absorption changes with an increase in dose and the position of the maximum shifts towards a longer wavelength of 476 nm (see curve 3 in Fig. 1b and curve 2 with respect to curve 1 in Fig. 1c). The position and the value of the maximum also depend on the type of impurity (358 nm and 2.5 cm^{-1} for A3 sample, curve 4 in Fig. 1c). It was found that annealing at room temperature for 8 months returned the optical characteristics to the initial type (curve 3 in Fig 1c). Similarly, annealing at 400°C for 3 h in air leads to the same effect (see curve 1 and curve 2 in Fig. 1b). Irradiation with gamma's performed at 77 K does not introduce new defects compared to 300 K (compare curve 4 and curve 3 in Fig. 1b).

Two samples of SLGO4 crystal (Fig. 2) were investigated after the next treatments: G1 as grown sample (pure SLGO4) was irradiated with γ 10^5 Gy at 300K in air (curve1). G2 as grown sample (Nd^{3+} doped - 2.5 at.% - SLGO4) was irradiated with γ 10^6 Gy in air (curve 2), annealed at 1200 °C and irradiated with γ 10^5 Gy in air (curve 3), next annealed in air for 3 h at 400 °C (curve 4) and irradiated with γ 10^5 Gy at 77 K (curve 5).

Pure SLGO4 crystal has the maximum value of additional absorption after γ 10^5 Gy at 415 nm (about 8 cm^{-1}, curve 1) but neodymium doped at 453 nm (about 8 cm^{-1}, curve 2). After annealing the crystal at 1200°C for 3 h the value of the maximum decreases (curve 3). Further annealing at 400°C of the γ-irradiated sample fully reconstructs absorption spectrum (curve 4). Irradiation of the crystal in liquid nitrogen temperature with the same value of the dose shifts the maximum towards longer wavelengths and decreases its value (curve 5).

The ESR lines observed by us in SLAO and SLGO4 crystals, called as „D"-defects (GLOUBOKOV et al. 1995), depend on the crystal coloration. Most intensive ESR lines were observed for dark-green single crystals and decreased for green and yellow crystals. For colorless crystals no ESR lines were measured.

After γ-irradiation of CNAO crystals (Fig. 2b) one wide additional absorption band is observed (see curve 1) with a maximum at 420 nm (12.5 cm^{-1}), which changes in intensity and position after subsequent thermal and radiation treatments. Annealing at 400°C shift the maximum towards a longer wavelength of 470 nm (curve 2). Subsequent γ-irradiation performed at 300 K and 77 K does not change position of the maximum (see curve3 and curve 4), but gives smaller values of additional absorption as compare to the first irradiation (curve 1).

4. LN and LT single crystals

Lithium niobate crystals doped by rare-earth and transition ions have attracted attention as self-frequency doubling and Q-switched lasers because of the possibility for combining the laser emission and non-linear properties of the matrix in a single medium.

Fig. 3. presents two possible kinds of doping of LN and LT single crystals: by diffusion (Fig. 3a, b) and during crystal growth (Fig. 3c). As seen from Fig. 3a most effective diffusion is observed in the case of LT crystal and for a temperature of 900°C. Diffusion process lead to a large increase in the optical density of the crystal in the UV range of a spectrum (Fig. 3b). Concentration of the impurity incorporated during diffusion increases with the duration of diffusion and an increase in a temperature (see Fig. 3a).

Doping during crystal growth with chromium introduces many point defects in the crystal (JABLONSKI et al. 1997) and is revealed after γ-irradiation as at least two additional

absorption bands at 381 nm and 464 nm; 15 cm^{-1} (Fig. 3c, curve 3). The second band suggests a recharging effect of chromium ions in the LN lattice. After electron or γ-irradiation of LN crystals doped with Cr, a new ESR spectrum having 3 anisotropy lines with Lande coefficient, g, equal to 2 is observed (see Fig. 3d). Moreover, irradiation of the crystals with electrons leads to a decrease in the intensity of Mn^{2+} lines (noncontrolled impurity) while γ-irradiation do not change this intensity (JABLONSKI et al. 1998 a).

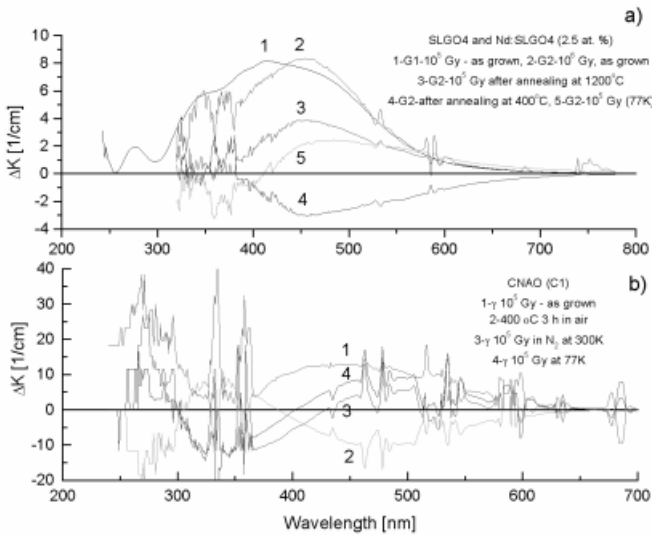

Fig. 2: Additional absorption in (a) pure (G1 sample) and Nd^{3+} (2.5 at.%) doped (G2) $SrLaGaO_4$ and (b) $CaNdAlO_4$ (C1 sample) single crystals after γ-irradiation with a dose of 10^5 Gy.

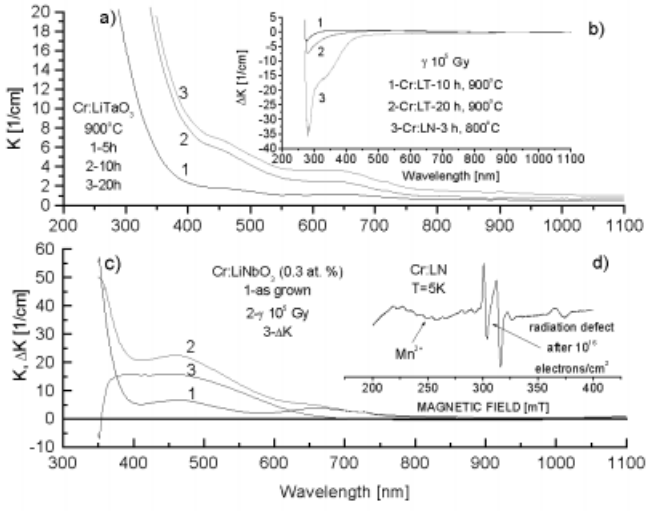

Fig. 3: (a) absorption, (b) additional absorption for $LiTaO_3$ and $LiNbO_3$ crystals doped by diffusion with Cr and Cu, respectively, after γ irradiation with a dose of 10^5 Gy, (c) absorption and additional absorption in $LiNbO_3$ crystals doped during growth with Cr after γ-irradiation with a dose of 10^5 Gy and, (d) ESR spectrum of Cr doped $LiNbO_3$ single crystal irradiated with electrons with a fluency of $5*10^{16}$ cm^{-2}

5. SLGO and BLGO crystals

ABC_3O_7 melilite crystals are characterized by relatively high structural homogeneity and good lasing properties. Undoped single crystals are successfully used as substrates for high temperature superconducting layers.

In BLGO and SLGO single crystals undoped and doped with rare eraths, both for gamma, electron and proton irradiation an intense (30 cm^{-1}) additional absorption band near 270 nm and, related with it, a new anisotropy ESR spectrum, marked as G1 - defect, was observed. Moreover, 370 nm band associated probably with oxide vacancies (KACZMAREK et al. 1998 a). Angular dependencies measured for different planes suggested that the observed lines are connected with oxide tetrahedral: four non-equivalent paramagnetic centers are seen. At room temperature these lines disappear after about 1 month from γ-irradiation. It was assumed that paramagnetic centers arises due to electron knock out from O^{2-} ion and further capture it by Ga^{3+} ion (KACZMAREK et al. 1998 a, JABLONSKI et al. 1998 b). This radiation defect leads to a shift in the fundamental absorption edge towards long wavelengths even by hundreds of nm (Fig. 4). As seen from the Fig. 4, for BLGO and SLGO crystals, the shift depends on the type of impurity (Fig. 4a, b), value of a dose (Fig. 4a curve 2 and curve 3), thickness of investigated sample (Fig. 4c) and, arises independent on type of the radiation (Fig. 4c - γ and Fig. 4d - protons, curves 2). Annealing of the crystals at 400°C for 3 h in air returned optical characteristics to type before irradiation (Fig. 4a, curve 4 and Fig. 4b, curve 3). The G1-type radiation defect was observed for BLGO and SLGO crystals undoped and doped with rare earths and transition ions, but did not arise in the case of $SrGdGa_3O_7$ crystals (KACZMAREK et al. 1998 b).

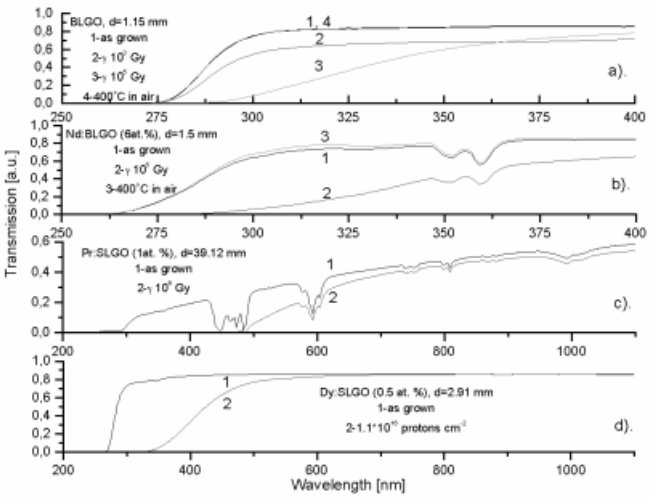

Fig. 4: Change in transmission of (a) undoped BLGO, (b) Nd: BLGO, (c) Pr: SLGO (c) and (d) Dy: SLGO single crystals after γ-rays (a-c) and protons (d)

6. YAG single crystals

YAG crystals are very often applied in optoelectronic devices as lasers and scintillate due to their good thermal and mechanical properties.

After γ-irradiation, pure and rare-earth doped YAG crystals show a wide, complex additional absorption band in the range between 200 and 900nm. Doping, for example, by neodymium weakly influences the shape of additional absorption band but cerium behaves inversely. Near 338 and 458 nm (transitions in cerium ions) the additional absorption bands arises that suggests recharging effect of cerium ions (KACZMAREK et al. 1998 c). Irradiation of the crystals in liquid nitrogen leads to grow of additional absorption bands even three times.

Fig. 5 presents additional absorption bands in pure YAG (Fig. 5a) and Ce, Nd: YAG (Fig. 5b) crystals after irradiation with protons with fluencies from 10^{12} to 10^{16} particles cm^{-2}.

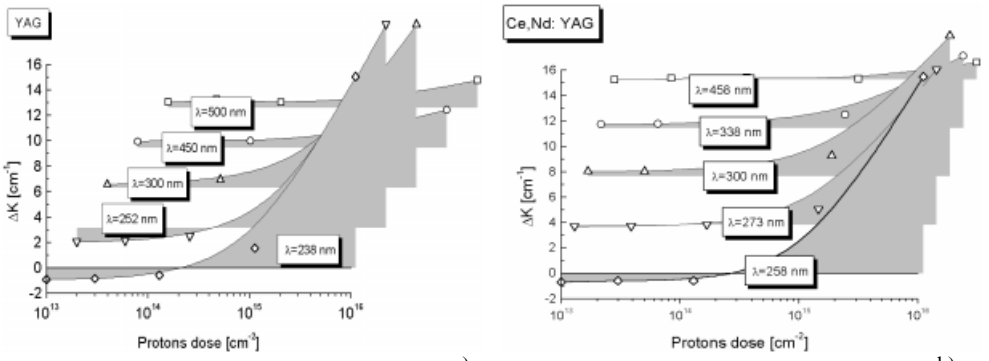

Fig. 5: Dose dependencies of proton irradiated (a) pure YAG and (b) Ce,Nd: YAG single crystals for several values of wavelengths and fluencies between 10^{12} and 10^{16} cm^{-2}

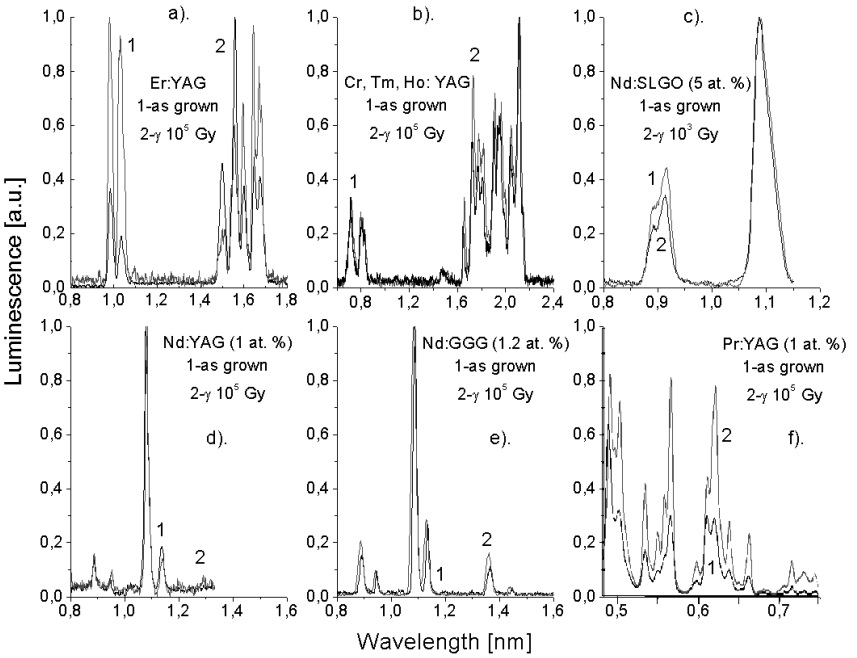

Fig. 6: Change in the luminescence of (a) Er: YAG, (b) Cr, Tm, Ho: YAG, (c) Nd: SLGO, (d) Nd: YAG, (e) Nd: $Gd_3Ga_5O_{12}$ and (f) Pr: YAG single crystals after γ-rays

From the figure two ranges on dose scale, dependent on the dose, can be distinguished: (1) fluencies less than $5*10^{14}$ cm^{-2} where recharging effects dominate and, (2) fluencies greater than $5*10^{14}$ cm^{-2} where the presence of Frenkel defects is clearly seen.

Fig. 6 presents changes in luminescence of YAG crystals doped with Er (Fig. 6a), Cr, Tm, Ho (Fig. 6b), Nd (Fig. 6d) and Pr (Fig. 6f) after γ-irradiation with a dose of 10^5 Gy. One can see large changes in Er: YAG (Fig. 6a) and Pr: YAG (Fig. 6f) crystals. In this figure changes in the luminescence spectrum after γ-irradiation of Nd doped SLGO and $Gd_3Ga_5O_{12}$ crystals are also seen for comparison (Fig. 6c, e). These changes are associated with the

presence of color centers (e.g. in Er: YAG - see KACZMAREK et al. 1996) that transfer energy of excitation to Er ions or valency change of active or sensitizing dopant (for example Ce or Cr in Ce: YAG or Cr, Tm, Ho: YAG crystals, respectively). The above mentioned changes in luminescence spectra have appropriate consequence in emission of lasers (KACZMAREK et al. 1997).

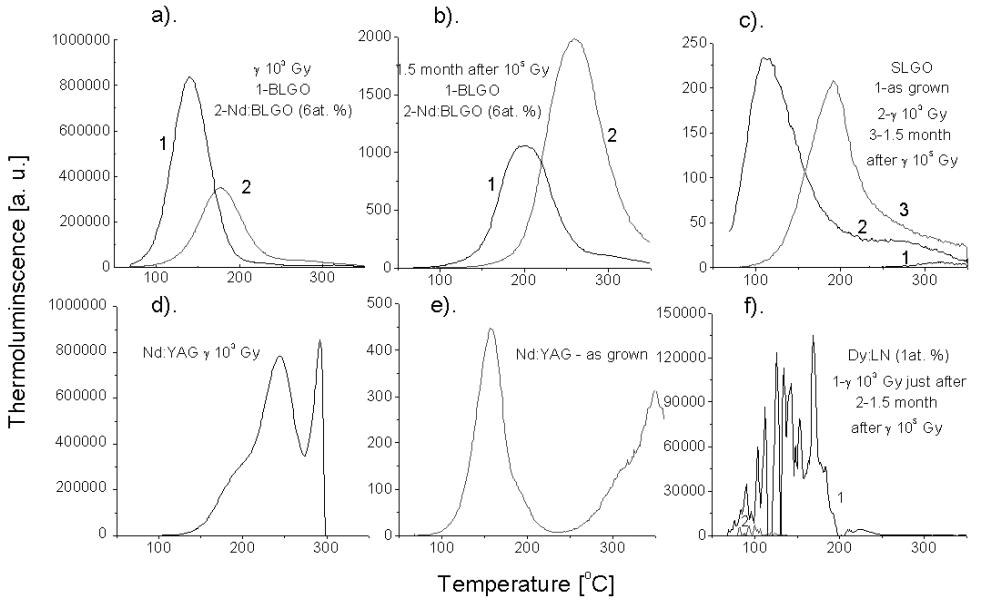

Fig. 7: Thermoluminescence of (a, b) BLGO and Nd: BLGO, (c) SLGO, (d, e) Nd: YAG, (f) Dy: LN single crystals after γ-irradiation with doses 10^3-10^5 Gy

7. Thermoluminescence and ESR measurements

Fig. 7 shows thermoluminescence measurements for BLGO and Nd: BLGO (curves 1 and 2 in Fig. 7a -after 10^3 Gy and curves 1 and 2 in Fig. 7b - 1.5 month after 10^5 Gy, respectively), SLGO (Fig. 7c - as grown crystal, curve 1, after 10^3 Gy, curve 2 and 1.5 month after 10^5 Gy, curve 3), Nd: YAG (Fig. 7d - after γ 10^3 Gy and Fig. 7e - for as grown crystal) and, Dy: LN (Fig. 7f - after 10^3 Gy, curve 1 and 1.5 month after 10^5 Gy, curve 2) single crystals. Radiation defects created in these crystals by gamma rays may be seen and their change with time (relaxation process). More strong radiation defect (measured as a maximum of thermoluminescence intensity) show BLGO and YAG crystals. YAG crystals exhibit at least two radiation defects while SLGO and BLGO crystals only one. Thermoluminescence of Dy: LN (Fig. 7f) crystal exhibit many narrow peaks. Comparing Figs 7a,b and 7c it may be seen the greater stability of radiation defects in SLGO than in BLGO crystals.

Fig. 8 illustrates the same radiation defects created in SLGO (Fig. 8a and b), BLGO (Fig. 8c) and Cr, Mn: LN (Fig. 8d) crystals observed by means of ESR technique. As seen from the figure radiation defect is revealed by new ESR lines (for example G1 line for SLGO, Fig. 8a), which relax with time (Fig. 8a,γ for SLGO and Fig. 8c for BLGO crystals) and whose intensity depends on the irradiation dose while shape on the temperature (Fig. 8b). Presented in Fig. 8 defects arises for all types of applied radiation, gammas (Fig. 8a,b,c) and electrons (Fig. 8d).

8. Summary

8.1 $ABCO_4$ single crystals

In the case of $ABCO_4$ crystals it has been found that the main reason of defects is oxygen vacancy. Some growth planes of crystals have similar value of the attachment energy and some of them contain great number of oxygen ions with weak bonding. Therefore, small changes of growth conditions affect the oxygen defects. After γ irradiation, in $ABCO_4$ single crystals additional absorption bands arise with a maxima at a level of 10 cm^{-1}, showing a tendency to change their shape and intensity with change of the dose. This means that investigated crystals are radiationally unstable.

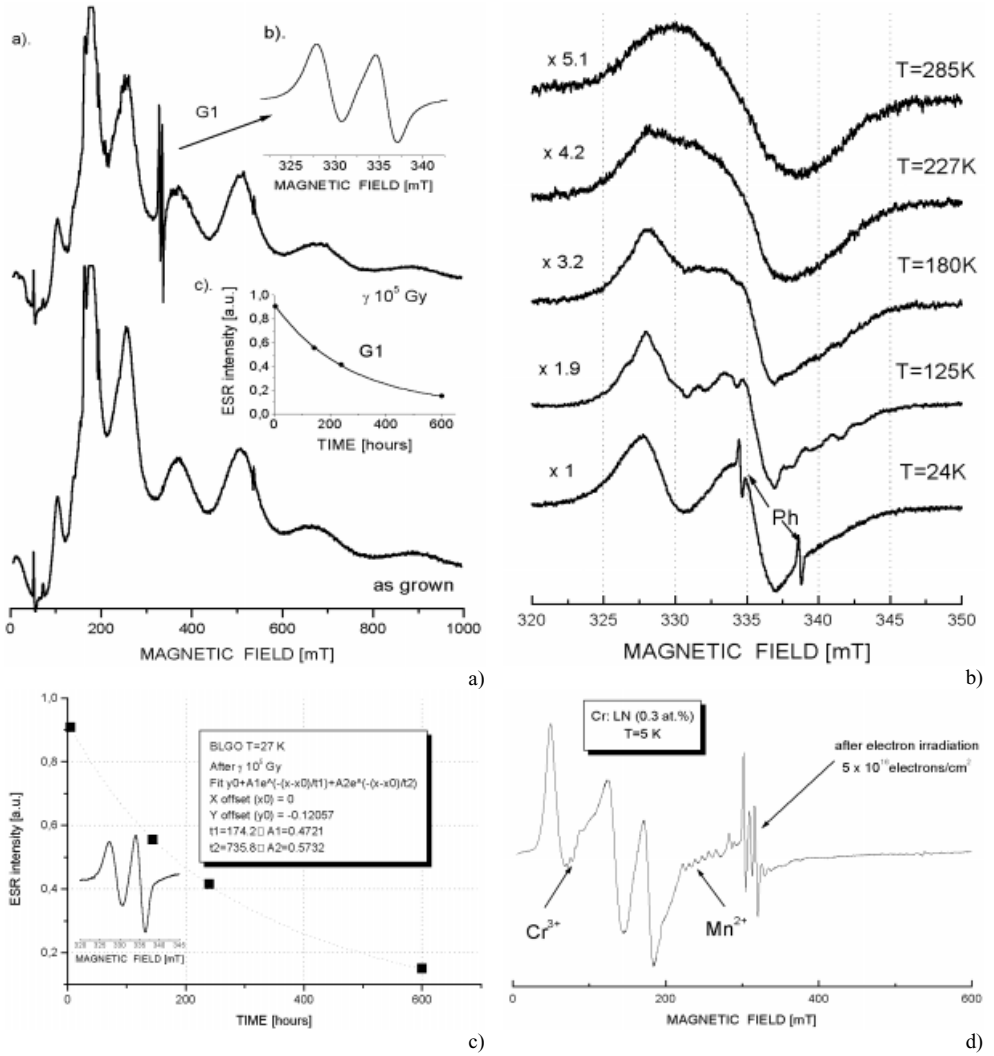

Fig. 8: ESR results in (a, b) SLGO, (c) BLGO and (d) Cr: LN single crystals after irradiation with gammas or electrons

8.2 LN and LT crystals

With the growth of impurity concentration the fundamental optical absorption edge remains unchanged (270 nm) for LT but changes for LN crystal doping by diffusion. Cr doping of these crystals by diffusion leads to an increase in the absorption density in the UV-range, while doping during crystal growth leads to an increase in the absorption density mainly in the VIS-range. Irradiation of the crystals with gammas leads to clearing of their absorption spectrum (-35 cm^{-1} for Cu: LN crystal), especially in the UV region, for LN crystals doped by diffusion and, to coloring (15 cm^{-1}), especially in the VIS region, for LN crystals doped during growth. This means that Cr doped by diffusion LN crystals exhibit lower level of defect content than doped during growth.

Doping during growth with chromium introduces many point defects and is revealed after γ-irradiation as at least two additional absorption bands at 381 nm and 464 nm. The second band suggests a recharging effect of chromium ions in the LN lattice. It is possible that Cr^{2+} ions are present in as grown crystals. This supposition is confirmed by a value of additional absorption (about 15 cm^{-1}) which suggests high level of defect content in the LN crystal.

After electron or γ-irradiation of LN crystals doped with Cr, a new ESR spectrum having 3 anisotropy lines is observed. Obtained by us angular dependencies are unambiguous due to the overlapping of Cr and paramagnetic peak lines. For this reason determination of peak localization was not possible.

8.3 SLGO and BLGO single crystals

In SLGO or BLGO crystals doped with Pr, Dy and Nd as well as undoped ones, after γ or proton irradiation, the additional absorption bands appear in the absorption spectra with the maxima at about 270 and 370 nm. The first band shifts the fundamental absorption edge of the crystal towards the longer wavelengths. This shifting depends on the type of impurity, irradiation dose and has similar character for gammas and protons for doses up to 10^6 Gy and fluency up to 10^{14} protons/cm^2, respectively. It also depends on the crystal thickness. We have shown that this optical effect is connected with paramagnetic G1 center placed in oxide tetrahedral around Ga^{3+} ion. It was assumed that paramagnetic centers arises due to electron knock out from O^{2-} ion and further capture it by Ga^{3+} ion, which stay paramagnetic Ga^{2+}.

8.4 YAG single crystals

After γ-irradiation, pure and rare-earth doped YAG crystals show a wide, complex additional absorption band (color centers) in the range between 200 and 900nm. The obtained by us results point to the direct influence of the color centers on the processes of formation of the inverse population of the energy levels of Er: YAG (positive), Cr, Tm, Ho: YAG (positive) and Nd: YAG (negative) lasers. Gamma irradiation leads to the create of color centers which transfer energy of excitation to excited laser level (as in the case of Er: YAG laser) and also to an increase in active impurity concentration and thus luminescence intensity, e.g. for Ce: YAG and Cr, Tm, Ho: YAG (Cr) crystals.

From additional absorption after proton irradiation performed on pure YAG and Ce, Nd: YAG crystals results that on dose scale, dependent on the dose, two ranges can be distinguished: (1) fluencies less than $5*10^{14}$ cm^{-2} where recharging effects dominate and, (2) fluencies greater than $5*10^{14}$ cm^{-2} where the presence of Frenkel defects is clearly seen. The same result we have obtained for SLGO crystals doped with Dy.

References

BEDILOV, M.R., BEISEMBAIEVA, H.B., SABITOV, M.S.: Kwantowa Elektronika, **21** (1994) 1145
GLOUBOKOV, A., JABLONSKI, R., RYBA-ROMANOWSKI, W., SASS, J., PAJACZKOWSKA, A., UECKER, R., REICHE, P.: J. Cryst. Growth, **147** (1995) 123
JABLONSKI, R., PRACKA, I., •WIRKOWICZ, M.: Proc. of SPIE, **3178** (1997) 303
JABLONSKI, R., KACZMAREK, S.M., PRACKA, I., SURMA, B., •WIRKOWICZ, M., LUKASIEWICZ., T.: Spectr. Acta A, (1998 a)
JABLONSKI, R., KACZMAREK, S.M., BERKOWSKI, M.: Spectr. Acta A, (1998 b), in print
KACZMAREK, S.M., MATKOVSKII, A.O., MIERCZYK, Z., KOPCZY•SKI, K., SUGAK, D.J.: Optoelectronics Review, **3/4** (1995) 74
KACZMAREK, S.M., MATKOVSKII, A.O., MIERCZYK, Z., KOPCZY•SKI, K., SUGAK, D.YU., DURYGIN, A.N., FRUKACZ, Z.: Acta Phys. Pol. A, **90** (1996) 285
KACZMAREK, S.M., KWA•NY, M., MALINOWSKI, M., MOROZ, Z.: Proc. SPIE, **3186** (1997) 51
KACZMAREK, S.M., .JABLONSKI, R., PRACKA, I., BOULON, G., LUKASIEWICZ, T., MOROZ, Z., WARCHO•, S.: Nucl. Instr. and Meth. in Phys. Research, (1998 a), in print
KACZMAREK, S.M., BERKOWSKI, M., JABLONSKI, R., PRACKA, I., KWA•NY, M., •WIRKOWICZ, M.: BIULETYN WAT, **7-8** (1998 b) 141
KACZMAREK, S.M., KISIELEWSKI, J., JABLONSKI, R., MOROZ, Z., KWA•NY, M., LUKASIEWICZ, T., WARCHO•, S., WOJTKOWSKA, J.: Biuletyn WAT, **7-8** (1998 c) 113
PAJACZKOWSKA, A.: Proc. of SPIE, **2373** (1995) 2

(received June 29, 1998; accepted August 26, 1998)

Authors' addresses:

Dr in•. S.M. KACZMAREK*
Institute of Optoelectronics
Military University of Technology
ul. Kaliskiego 2, 00-908 Warsaw, Poland

Dr R. JABLONSKI, mgr I. PRACKA, Prof. dr hab. T. LUKASIEWICZ
Institute of Electronic Materials Technology
ul. Wólczy•ska 133, 01-919 Warsaw, Poland

Prof. dr hab. Z. MOROZ
Soltan Institute of Nuclear Studies
05-400 •wierk, Poland

*Corresponding author:
e-mail: skaczmar@wat.waw.pl.; FAX: 666 89 50